15th Australasian Fluid Mechanics Conference
The University of Sydney, Sydney, Australia
13-17 December 2004

Turbulence Models and Boundary Conditions for Bluff Body Flow

M. E. Young[1] **and A. Ooi**[2]

[1]Flight Systems Branch, Air Vehicles Division, Defence Science and Technology Organisation
Fishermans Bend, Victoria, 3207 AUSTRALIA

[2]Department of Mechanical and Manufacturing Engineering
Melbourne University, Victoria, 3000, AUSTRALIA

Abstract

Two aspects of turbulence modelling were addressed with respect to a single cylinder in crossflow. Firstly, the effect of varying the turbulent length scale at the inlet was investigated at a high subcritical Reynolds number of 1.4×10^5. Variations of up to 14% were noted in the flow properties such as mean drag and Strouhal number, but significant discrepancy between experimental and computational results remained. Secondly, a modification to the standard k-ω turbulence model was assessed. This time-limit model modified the turbulent viscosity term, inhibiting production of turbulent kinetic energy in areas of high strain rates. Tuning of an empirical term was required to match flows at various Reynolds numbers. The time-limit model appeared to offer improvements at some Reynolds numbers compared to the standard k-ω model by reproducing real flow structures such as separation bubbles at a transcritical Reynolds number. Use of the time-limit model is in its infancy, especially in unsteady flows, but appears to have some potential.

Introduction

The complex nature of the flow around a cylinder makes it an excellent case to assess the ability of computational packages to reproduce real flow conditions. At very low Reynolds numbers, the flow around a cylinder is symmetric and steady. As the Reynolds number is increased, asymmetric vortex shedding occurs. This shedding is periodic, therefore requiring an unsteady time dependent solution. The non-dimensional frequency of the vortex shedding is represented by the Strouhal number. The shedding alters the wake behind the cylinder and impacts on the flow properties: drag and lift are now periodic and the mean drag changes from the steady solution. At higher Reynolds numbers, as investigated here, the wake or boundary layer becomes turbulent — requiring a turbulence model. Two-equation models such as the k-ω and k-ε families offer the ability to introduce turbulence into a flow with minimal additional computational overhead.

This paper assesses the ability to computationally predict the mean flow parameters around a bluff body. The accurate prediction of flow parameters such as drag coefficient and Strouhal number hinges on accurate calculation of the separation point. This is because, in broad terms, the point of separation will generally define the width of the wake which, in turn, is a major contribution to the drag experienced by a body.

The two-equation eddy-viscosity turbulence models as used in this paper require two boundary conditions. The first is satisfied by the turbulence intensity, I (or by turbulent kinetic energy, k which is related to I by $k = 3/2(U_{avg}I)^2$). Experimental studies will generally provide an estimate of the upstream turbulence intensity ($I = Tu = \overline{u'^2}^{1/2}/u_\infty$) that has been measured in the experimental facility. The second boundary value can be posed in various ways such as turbulent length scale, l; dissipation terms, ω or ε; or viscosity ratio, $r_\mu = \mu_t/\mu$. However, these values are often not available, and must therefore be estimated. Tutar and Holdø [9] assume a single value for turbulent length scale based on various suppositions. Other papers by Bosch and Rodi [1], and Lakehal and Thiele [6] look at variations in l to a limited degree. These studies found that the variation in turbulence conditions at the inlet had a marked effect on the flow. The current study aims to compare the estimated flow properties and flow field about a single cylinder using the k-ω Shear Stress Transport (k-ω SST) turbulence model for a range of turbulent inlet conditions.

The study of bluff body flow was continued by introducing the time-limit turbulence model modification as proposed by Durbin [3]. The new model purportedly addresses one of the shortcomings of two-equation turbulence models, that of overproduction of turbulent kinetic energy. Application of the time-limit model to unsteady flows has been limited and therefore the results presented are largely of an exploratory nature.

Numerical Model

The unsteady Reynolds-averaged Navier Stokes equations were solved using the commercial CFD code Fluent (version 6.1.22, [5]). Variations of the k-ω two-equation eddy-viscosity turbulence models were used, with Menter's [8] k-ω SST model being used for part one of this study. This model offers improved performance with respect to adverse pressure gradients. It was chosen to fully resolve the boundary layer thereby requiring the quadrilateral mesh be created such that $y+ = yu_\tau/\nu$ was less than one. This required the distance from the wall to the first grid point, y, to be between $0.01\%D$ (for Reynolds numbers 10^3 and 1.4×10^5) and $0.0005\%D$ ($Re = 3 \times 10^6$). The stretching ratio for the mesh was approximately 1.08 in most instances and less than 1.1 in all cases. The meshed domain is presented in figure 1. The upstream boundary was defined as a velocity inlet, allowing inflow velocity and the two turbulence boundary conditions to be defined. The downstream boundary was modelled as a simple outflow. The lateral boundaries were defined such that there was zero normal velocity and zero normal gradients.

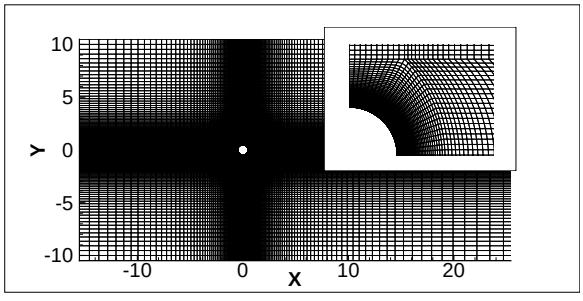

Figure 1: Computational domain arrangement, with detail of the mesh close to the cylinder. Inlet is at $x = -15.5D$; outlet is at $x = 25.5D$; and lateral boundaries are at $y = \pm 10.5D$.

Cantwell and Coles [2] note that the freestream turbulence intensity in their tunnel was less than or equal to 0.6%. Therefore, turbulence intensity, I, was set to 0.6% at the inlet. There is no data on the appropriate length scale in [2] and this must therefore be estimated on the basis of other arguments. As outlined in the introduction, [1] and [6] have noted that selection of different length scale boundary conditions does impact the subsequent flow downstream, and hence this formed the focus of the first part of this study.

Solutions were instigated by developing the flow in the steady solver before introducing an asymmetric perturbation into the flow. The unsteady solver was used subsequent to the introduction of the disturbance, ensuring the timestep was of the order of one hundredth of the expected period (known from experimental measurement of Strouhal number: $\Delta t = 0.01D/(StU)$). The transients resulting from the perturbation were allowed to exit the domain before any data was recorded. To ensure the solution was independent of the starting conditions (i.e. the perturbation), a case was run allowing the asymmetry to grow naturally over time. This gave the same flow properties ($\overline{C_D}$ and St) as the result obtained by perturbing the flow artificially. Mesh independence was tested with higher density meshes in both the radial and tangential directions, and resulted in variations in the mean flow parameters of less than 1 percent. The mean flow conditions were obtained by time-averaging the flow over three periods once the transients had exited the domain.

The same mesh and procedure was used to assess the time-limit model. However, the standard k-ω model (Wilcox [10]) was used as the basis for the time-limit modification.

The two-dimensional formulation of Durbin's time-limit turbulence model is briefly presented here (see [3]). Consider the turbulent viscosity in the form:

$$\mu_t = C_\mu \rho u^2 T \tag{1}$$

In the standard k-ω model, the velocity scale u^2 is equal to k, and the timescale, $T = 1/(C_\mu \omega)$. A timescale bound is developed in [3] by applying a realizability constraint in order to ensure that the square of the normal components of the Reynolds stress tensor are always positive. This defines the timescale in the two-dimensional case thus:

$$T \leq \frac{2k}{3u^2 C_\mu} \frac{1}{\sqrt{2|S|^2}} \tag{2}$$

Durbin [3] suggests that an empirical constant of value less than one may be used in order to tune the model to experimental flows. This constant was expressed as α in Medic and Durbin [7]. Therefore, reducing (2), gives

$$T \leq \frac{\sqrt{2}\alpha}{3C_\mu |S|} \tag{3}$$

or, for a computational application:

$$T = \min\left[\frac{1}{C_\mu \omega}, \frac{\sqrt{2}\alpha}{3C_\mu |S|}\right] \tag{4}$$

The time-limit modification was included through a user defined function that defined the turbulent viscosity by using equation (4) in equation (1).

Results and Discussion

Turbulent Inlet Boundary Conditions

To investigate the effect of the turbulent length scale boundary condition, the length scale was varied by orders of magnitude from $l = 0.0001D$ to $0.1D$. Various mean and fluctuating flow properties have been compared with the study of Cantwell and Coles [2]. Table 1 summarises the results from the present study and table 2 presents experimental data from [2], as well as additional computational results from [9]. $\widetilde{C_D}$ and $\widetilde{C_L}$ are the periodic fluctuations in the force coefficients.

Length scale	$r_\mu = \mu_t/\mu$	$\overline{C_D}$	St	$\widetilde{C_D}$	$\widetilde{C_L}$
0.1D	102.9	0.692	0.238	0.0074	0.297
0.05D	51.4	0.685	0.248	0.0096	0.327
0.01D	10.3	0.729	0.260	0.0204	0.470
0.001D	1.03	0.799	0.257	0.0363	0.671
0.0001D	0.103	0.776	0.258	0.0348	0.642

Table 1: Results of varying turbulent length scale ($Re = 1.4 \times 10^5$, $I = 0.6\%$).

Study	Length scale	$\overline{C_D}$	St	$\widetilde{C_L}$
Exp. [2]	n/a	1.237	0.179	n/a
k-ε [9]	0.02D	0.71	-	-
RNG k-ε [9]	0.02D	0.98	0.167	0.51
LES [9]	0.02D	1.40	0.184	0.65

Table 2: Experimental and computational results ($Re = 1.4 \times 10^5$, $I = 0.6\%$).

The present study's results underestimate mean drag coefficient and overestimate Strouhal number. Similarly, the k-ε results from [9] also underestimate $\overline{C_D}$, however the standard k-ε model does not predict any vortex shedding, and the RNG model underpredicts Strouhal number. The large eddy simulation (LES) results from [9] provide a closer match to experiment.

Figure 2 presents the distribution of pressure coefficient about the cylinder. On the front side of the cylinder, the reduction in pressure in the experimental data is small in comparison to the computational predictions, and the experimental results indicate an earlier separation point. The computational results are quite similar in this region except at the low pressure minima, where smaller length scales predict a lower pressure coefficient. The predominant difference between the pressure distributions predicted with the use of varying length scales is the different base pressures on the aft side of the cylinder. [2] cites a base pressure coefficient of -1.21. In this region, the small length scales offer an improved match — the closest computational result is for $l = 0.001D$, with a value of -0.918, which is markedly better than for $l = 0.1D$ where C_{p_b} = -0.637.

It is suggested that the improvement in estimation of the C_p distribution on the aft side of the cylinder can be attributed to the fact that, with greater length scales, the flow has higher eddy viscosity according to the relationship $\mu_t = \rho k^{1/2} l$. This increased viscosity results in a higher velocity gradient at the wall, energising the boundary layer and consequently delaying separation.

The results presented here cover length scales over a range of four orders of magnitude, with the predicted $\overline{C_D}$ values varying -7 to +8.5% of the value averaged across all length scales. Strouhal number varies -5.6 to +3.1%. This suggests that the selection of length scale has only limited implication on the overall time-averaged flow properties. That is, incorrect estimation of length scale by an order of magnitude does not nec-

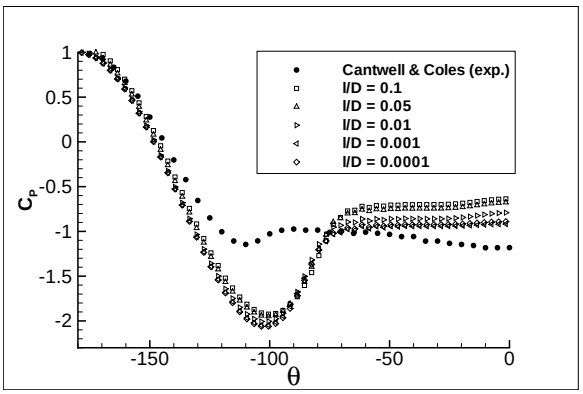

Figure 2: A comparison of the C_p distributions for different length scales at $Re = 1.4 \times 10^5$.

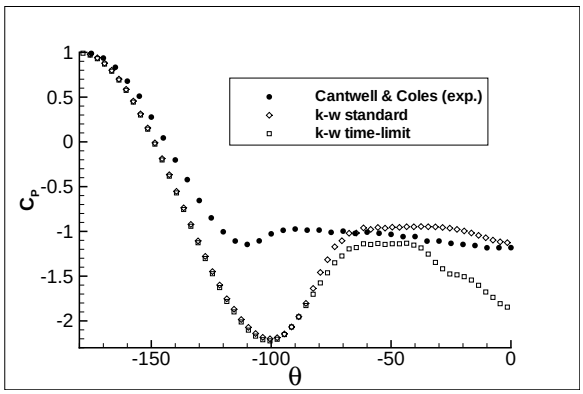

Figure 3: A comparison of the C_p distribution of different turbulence models at $Re = 1.4 \times 10^5$.

essarily convey with it a result that is in error by a similar order. However, this is contingent on the fact that the model in use is capable of accurately predicting the flow. For the cylinder in crossflow as presented here, the poor showing of computational results cannot be attributed to selection of incorrect length scale. Therefore, further improvements need to be made on the modelling of such flows.

Time-Limit Turbulence Model Modification

Durbin [3] proposed this modification (referred to as a time-scale bound) for eddy-viscosity turbulence models to overcome the tendency for overprediction of turbulent kinetic energy, *k*, around the stagnation point - the so-called stagnation point anomaly. Durbin proposed that it is not the stagnation point as such, but the large strain rates at this location, that result in the overproduction of *k*.

The time-limit model was first implemented in this study for the same $Re = 1.4 \times 10^5$ case as used above and it was found that the flow was very sensitive to the value of α, dramatically varying the entire flow structure such that mean drag varied from approximately 0.2 to 1.2.

When used with $\alpha = 0.7$ at $Re = 1.4 \times 10^5$, it was found that the model gave an improved estimation of drag coefficient, $\overline{C_D} = 1.223$ compared to 1.237 in [2]. However, further investigation revealed that this is not due to correct modelling of the flow. In fact, the mechanism for the high drag was not early separation together with a wide wake (as seen experimentally at this Reynolds number), but late separation in combination with a very low base pressure region. Figure 3 illustrates the variations in pressure distribution between the experimental data, the standard *k*-ω model and the time-limit model, for which the low base pressure at $\theta = 0$ is evident.

Figure 4 illustrates the regions in which the modified time-scale and conventional *k*-ω formulations are active. In the modified time-scale region the turbulent viscosity was noted to be greatly reduced compared to the standard *k*-ω model. This resulted in a reduction in the turbulence intensity around the cylinder as seen in figure 5.

The time-limit model was subsequently tested over a range of Reynolds numbers from 10^3 to 3×10^6. Figure 6 illustrates the trend in drag coefficient and Strouhal number across the Reynolds number range. Data computed using the standard *k*-ω model can be seen plotted in the figure, showing a negative, almost log-linear relationship as *Re* increases, but not capturing the reduction in drag nor subsequent drag increase. Using the time-limit model with $\alpha = 0.7$, the CFD still does not capture

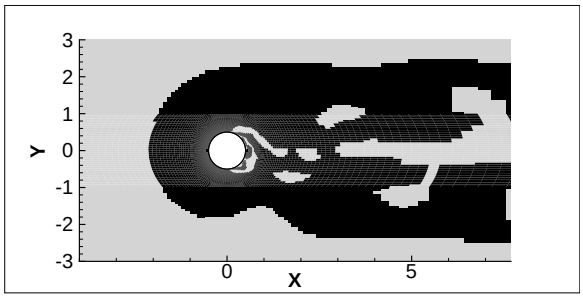

Figure 4: Representation of where the time-limit model is activated (dark region).

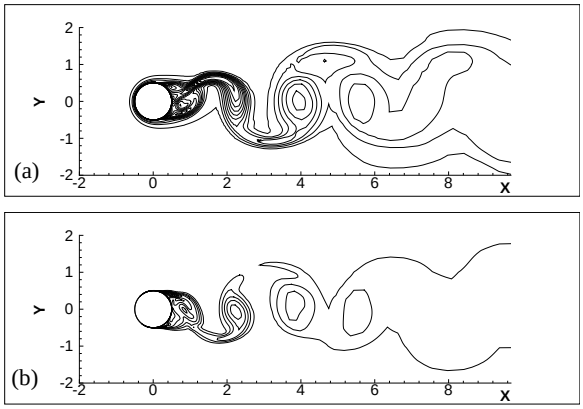

Figure 5: A comparison of the turbulence intensities — (a) *k*-ω standard, (b) *k*-ω time-limit. Contours are from 2% to 24% in increments of 2%.

the drag crisis, although it does give improved results either side of the critical region. By changing the empirical constant, α, to a value of 0.433, the low drag values at the critical Reynolds number of 5×10^5 can be modelled. This is of significance because the flow structure appears to match that seen in experiments. This can be seen in figure 7b where the separation bubble can be seen on the aft side of the time-limit model, which delays separation resulting in a narrower wake.

Figure 8 compares the pressure distribution about the cylinder at critical Reynolds numbers where the computational result at $Re = 5 \times 10^5$ is compared with experimental data from Farell and Blessman [4] at $Re = 3.8 \times 10^5$ – both in the critical Reynolds number regime according to figure 6.

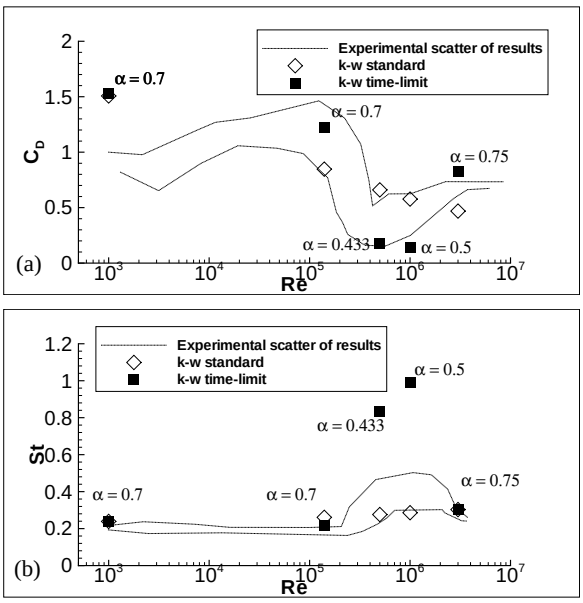

Figure 6: Experimental and computational results of (a) mean drag coefficient, and (b) Strouhal number, on a cylinder in cross-flow at various Reynolds numbers.

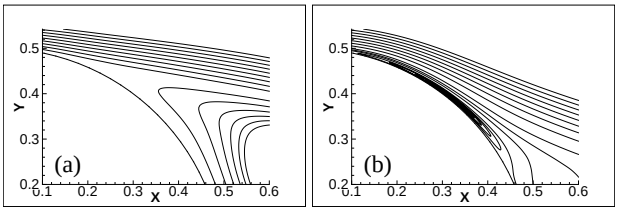

Figure 7: Detail of the flow structure around a cylinder at $Re = 5 \times 10^5$ — (a) k-ω standard, (b) k-ω time-limit.

Both the standard and time-limit model compare well with the experimental pressure distribution on the forward part of the cylinder. The low pressure peak is slightly too high for the standard model, and slightly too low for the time-limit model. The pressure in the wake of the standard model is lower than the experimental data whilst the time-limit model overpredicts the pressure recovery.

As Reynolds number exceeds 1×10^6, the transcritical regime is being approached and experimental results (refer figure 6) suggest the drag should begin to increase. This result was not obtained with the time-limit model. It was found that at $Re = 1 \times 10^6$ (using $\alpha = 0.5$), the time-limit model predicted a similar flow structure as at $Re = 5 \times 10^5$ but with lower drag.

When applied with $\alpha = 0.75$, the time-limit model gave a reasonable match with experimental data at $Re = 3 \times 10^6$, where it estimated a drag coefficient of 0.822.

Conclusions

It was found that the variation in flow parameters such as mean drag coefficient and Strouhal number were influenced by changes in the turbulent boundary conditions. However, large changes in turbulent length scale of several orders of magnitude did not translate into variations of the same magnitude in the measured flow properties. The performance of CFD was quite poor regardless of the chosen boundary conditions, and it is evident that improvements to eddy-viscosity modelling are required for such bluff body flows at high subcritical Reynolds numbers. The time-limit turbulence model modification appears to offer some improvement over the standard k-ω model, especially in its ability to correctly model some flow structures. However, this improvement is contingent on operation at suitable Reynolds number and the chosen α values.

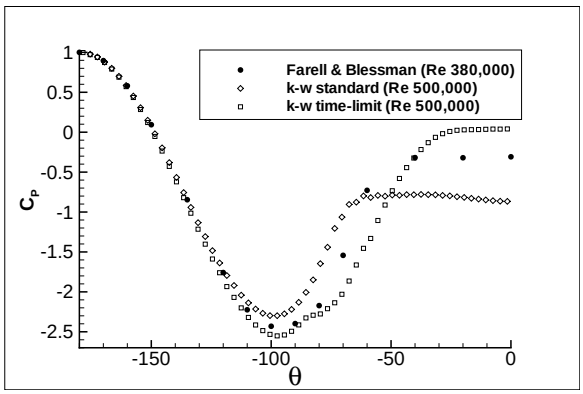

Figure 8: Comparison of pressure coefficient distribution about the cylinder in the critical Reynolds number regime.

Acknowledgements

This work was supported by DSTO and the authors would like to thank Jan Drobik and Greg McKenzie for their assistance.

References

[1] Bosch, G. and Rodi, W., Simulation of Vortex Shedding Past a Square Cylinder With Different Turbulence Models, *Int. J. Numer. Meth. Fluids*, **28**, 1998, 601–616.

[2] Cantwell, B. and Coles, D., An Experimental Study of Entrainment and Transport in the Turbulent Near Wake of a Circular Cylinder, *J. Fluid Mech.*, **136**, 1983, 321–374.

[3] Durbin, P.A., On the k-3 Stagnation Point Anomaly, *Int. J. Heat and Fluid Flow*, **17**, 1996, 89-90.

[4] Farell, C. and Blessman, J., On Critical Flow Around Smooth Circular Cylinders, *J. Fluid Mech.*, **136**, 1983, 375–391.

[5] Fluent Inc. *FLUENT 6.1 User's Guide*, Fluent Inc., Lebanon, USA, 2003.

[6] Lakehal, D. and Thiele, F., Sensitivity of Turbulent Shedding Flows to Non-Linear Stress-Strain Relations and Reynolds Stress Models, *Computers and Fluids*, **30**, 2001, 1–35.

[7] Medic, G. and Durbin, P.A., Toward Improved Prediction of Heat Transfer on Turbine Blades, *Journal of Turbomachinery*, **124**, 2002, 187–192.

[8] Menter, F.R., Two-Equation Eddy-Viscosity Turbulence Models for Engineering Applications, *AIAA Journal*, **32**, 1994, 1598–1605.

[9] Tutar, M. and Holdø, A.E., Computational Modelling of Flow Around a Circular Cylinder in Sub-critical Flow Regime with Various Turbulence Models, *Int. J. Numer. Meth. Fluids*, **35**, 2001, 763–784.

[10] Wilcox, D.C., *Turbulence Modelling for CFD*, DCW Industries, La Cañada, 1998.